scientific reports

Check for updates

OPEN

mTOR/HIF-1α-associated scleral metabolic reprogramming by Mingshi formula in form-deprivation myopia

Yixue Yin[1,2,3,4], Xiuyan Zhang[1,2,3,4], Yibo Han[2], Jike Song[1,2,3,4]✉ & Hongsheng Bi[1,2,3,4]✉

Focusing on the mTOR-HIF-1α signaling pathway, this study investigated the mechanism through which the traditional Chinese medicine compound Mingshi Formula delays the progression of form-deprivation myopia (FDM) in guinea pigs. The guinea pigs were divided into the normal control group (NC), FDM group, Mingshi Formula low-dose group (FDM + Low), medium-dose group (FDM + Medium), high-dose group (FDM + High), and MTOR inhibitor group (FDM + RapaLink-1). The guinea pig model of FDM was established by applying 3D-printed hoods modified by a latex balloon with 60% light transmission for 4 weeks. Refractive error changes were monitored using a refractometer. Axial length was quantitatively analyzed using A-scan ultrasound, choroidal thickness was measured with SD-OCT, and structural changes of the choroid and sclera were observed after hematoxylin-eosin (HE) staining. At the molecular level, the expression levels of the mammalian target of rapamycin (mTOR), phosphorylated mTOR (p-mTOR), HIF-1α, LDHA, PKM2, MMP2, Collagen I, and α-SMA in the sclera were measured by RT-qPCR and Western blotting. The spatial distribution characteristics of mTOR, p-mTOR, HIF-1α, and Collagen I were verified via immunofluorescence techniques. The results demonstrated that the Mingshi Formula significantly decreased myopic refractive error and axial length ($p < 0.01$), increased choroidal thickness ($p < 0.05$), downregulated the gene and protein expression of mTOR, p-mTOR, HIF-1α, LDHA, PKM2, MMP2, and α-SMA in response to hypoxia, and upregulated the expression of Collagen I compared to the FDM group. We demonstrated that MingShi formula modulates the mTOR/HIF-1α signaling axis to ameliorate scleral hypoxic metabolic homeostasis, regulate Collagen synthesis, inhibit aberrant extracellular matrix remodeling, and ultimately delay myopia progression.

Keywords Myopia, Mingshi formula, mTOR-HIF-1α, Phosphorylation, Scleral hypoxia

Abbreviations

FDM	Form-deprivation myopia
FDM + Low	Mingshi Formula low-dose group
FDM + Medium	Mingshi Formula medium-dose group
FDM + High	Mingshi Formula high-dose group
HE	Hematoxylin-eosin
mTOR	Mammalian target of rapamycin
p-mTOR	Phosphorylated mammalian target of rapamycin
ECM	Extracellular matrix
HIF-1α	Hypoxia-inducible factor-1α
SD-OCT	Spectral-domain optical coherence tomography
SDS-PAGE	Sodium dodecyl sulfate-polyacrylamide gel
PVDF	Polyvinylidene fluoride

[1]Affiliated Eye Hospital of Shandong University of Traditional Chinese Medicine, Jinan 250002, China. [2]Medical College of Optometry and Ophthalmology, Shandong University of Traditional Chinese Medicine, Jinan 250355, China. [3]Shandong Provincial Key Laboratory of Integrated Traditional Chinese and Western Medicine for Prevention and Therapy of Ocular Diseases, Jinan 250002, China. [4]Shandong Academy of Eye Disease Prevention and Therapy, Jinan 250002, China. ✉email: edusjk@163.com; hongshengbi1@163.com

Myopia is the most common refractive error worldwide, whose progression is significantly and positively correlated with pathological axial elongation. Epidemiological data showed that the prevalence of high myopia (≤-6.00 D) among adolescents has increased by 217% over the past decade[1]. Hypoxia-driven imbalance in the homeostasis of the extracellular matrix (ECM) in the sclera has been identified as a core pathological factor involved in axial elongation[2]. Under hypoxic stress, hypoxia-inducible factor-1α (HIF-1α) in scleral fibroblasts binds to hypoxia response elements, thereby transcriptionally activating target genes, such as α-SMA and MMP2. Activation of these target genes leads to an imbalance in collagen synthesis and degradation, resulting in the thinning and disorganization of collagen fibers, ECM degradation, and decreased biomechanical strength of the sclera, finally promoting axial elongation. However, the mechanisms underlying HIF-1α-mediated myopia remain largely unknown.

In form-deprivation myopia (FDM), scleral hypoxia and ECM remodeling represent key pathological hallmarks in the pathogenesis[3]. Recent studies demonstrate that mTOR phosphorylation is activated in myopic sclera, where it interacts with HIF-1α to drive downregulation of type I collagen (Collagen I) in scleral fibroblasts and promote myofibroblast transdifferentiation, thereby contributing to myopia development[2]. Consequently, targeting the mTOR/HIF-1α signaling axis represents a promising therapeutic strategy for myopia intervention. The mTOR, a key regulator of metabolism, is regulated by HIF-1α in a bidirectional manner: hypoxia not only induces mTOR phosphorylation (p-mTOR Ser2448) through the PI3K/Akt pathway but mTOR also enhances the transcriptional activity of HIF-1α, thereby forming a "hypoxia-metabolism" positive feedback loop that exacerbates abnormalities[4,5]. However, the regulatory mechanisms by which the mTOR/HIF-1α signaling pathway is involved in scleral ECM homeostasis, especially its interaction with HIF-1α, remain poorly understood.

Clinical studies have shown that Mingshi Formula (Ming's), a clinically validated traditional Chinese medicine compound used for controlling myopia, can significantly decelerate the progression of low myopia refractive error in adolescents and effectively control abnormal axial elongation[6]. Scleral metabolomics and pharmacological studies have suggested that Ming's Formula exerts multi-targeted interventions on the scleral hypoxic microenvironment, extracellular matrix (ECM) remodeling, and metabolic reprogramming, including the MMP2, mTOR, and HIF-1α signaling pathways, purine metabolism, and amino acid metabolism[7]. However, the specific underlying mechanisms need further studies. Notably, Core components in Ming's Formula (e.g., ginsenosides and gastrodin) have been documented to modulate cellular metabolic processes through regulation of the mTOR and HIF-1α signaling pathways. Suah as, Ginsenosides mediate anti-tumor activity by regulating the mTOR/HIF-1α signaling pathway, and also suppress autophagy via the PI3K/Akt/mTOR signaling pathway, thereby reducing myocardial ischemia[8,9]. Gastrodin could protect against H/Rhypoxia/reoxygenation injury of myocardial cells in neonatal rats by reducing the level of autophagy through the activation of mTOR signals in PI3K-Akt pathway[10]. These findings suggest that Ming's Formula likely mediates regulatory effects on scleral metabolism by targeting the mTOR/HIF-1α signaling axis.

This study aimed to establish an FDM guinea pig model to measure mTOR expression and its phosphorylation levels, detect scleral hypoxia-related indicators, and investigate the effects of Ming's Formula on their expression. We aimed to explore how Ming's Formula controls axial elongation and delays the progression of myopia, thereby offering a new theoretical basis for the application of Ming's Formula in the prevention and treatment of myopia.

Materials and methods

Animals

This study included 75 healthy 2-week-old male tricolor short-haired guinea pigs of the British strain. They were purchased from Jinan Jinfeng Laboratory Animal Co., Ltd., with an initial body weight of 130 ± 10 g. All guinea pigs were housed in standard laboratory animal facilities, where the ambient temperature was maintained at 22–25 °C and relative humidity was controlled at 50–60%, with a 12-hour light/dark cycle. During the experiment, the guinea pigs had free access to sterilized drinking water and were fed fresh vegetables and standardized nutritional feed. Before starting the experiment, all guinea pigs underwent comprehensive ophthalmic examinations, including slit-lamp microscopy and fundus examination to exclude congenital or acquired eye diseases (e.g., cataracts, glaucoma, or retinal pathologies). All experimental protocols involving animals were reviewed and approved by the Ethics Committee of the Affiliated Hospital of Shandong University of Traditional Chinese Medicine (Approval No.2023010) and strictly followed the ARRIVE (Animal Research: Reporting of In Vivo Experiments) guidelines.

Ninety guinea pigs were randomly divided into six groups, as follows ($n = 15$ per group): normal control (NC), form-deprived myopia (FDM) model, Ming's Formula low-dose group (FDM + Low), Ming's Formula medium-dose group (FDM + Medium), Ming's Formula high-dose group (FDM + High) and MTOR inhibitor group (FDM + RapaLink-1). The composition of Ming's Formula was as follows: 2 g Panax ginseng, 8 g Poria cocos, 5 g Dioscorea opposita, 5 g Polygala tenuifolia, 5 g Acorus tatarinowii, 5 g Polygonatum sibiricum, 5 g Salvia miltiorrhiza, and 5 g Gastrodia elata, which were provided by Beijing Kangrentang Pharmaceutical Co., Ltd.). The right eye of each guinea pig was used as the experimental eye, whereas the left eye served as the internal control. The NC group was kept under standard conditions and received no intervention. The FDM group, Ming's Formula groups and inhibitor group wore the 3D-printed hoods (modified by a latex balloon with 60% light transmission) on the right eye, leaving the left eye, nose, mouth, and ears exposed.

The dosage of Ming's Formula was determined based on the "Human-Guinea Pig Body Surface Area Equivalent Dose Conversion Principle" as described in the "Methodology of Pharmacological Experiments in Traditional Chinese Medicine." The low-dose, medium-dose, and high-dose groups received 0.5, 1.0, and 1.5 times the clinical equivalent dose, corresponding to 0.33 g/kg, 0.65 g/kg, and 1.3 g/kg doses, respectively, and the inhibitor group received 1.5 mg/kg dose of RapaLink-1. After establishing the model, the Ming's Formula was administered via daily oral gavage and continued for 4 weeks until sacrifice, and weekly weighed to adjust the

dosage. And the inhibitor group received intraperitoneal injections of RapaLink-1 administered once every 10 days for a total of three doses, with doses adjusted weekly according to body weight. The integrity of the hoods of the guinea pigs in each group was monitored twice daily (morning and evening), and any detached or damaged eye patches were promptly replaced.

Measurement of ocular parameters

The refractive error of all experimental guinea pigs was measured using a refractometer (Striatech GmbH, Germany) at baseline and 4 weeks after modeling. Before measurement, all animals were placed in a dim environment for dark adaptation, and then one drop of 0.5% compound tropicamide eye drop (Shenyang Xingqi Ophthalmology Company) was administered to both eyes three times, with a 10-minute interval between two doses. The examination was conducted 15–20 min after the last dose, with a working distance of 50 cm. The refractive error was calculated as the average of the vertical and horizontal principal meridians. The axial length was measured using an ultrasound system (Chongqing Wangguo Medical Instrument Co., Ltd., China). Before measurement, the probe surface was cleaned with anhydrous ethanol, and all guinea pigs were anesthetized with 0.4% oxybuprocaine hydrochloride (Santen Pharmaceutical Co., Ltd., Japan). The probe was carefully placed perpendicular to the corneal apex, aligned with the center of the pupil without compressing the cornea. Each eye was examined 10 times consecutively, and the average value was recorded. The entire measurement process was conducted by the same experienced technician.

Measurement of choroidal thickness

Quantitative evaluation of choroidal thickness in the central region of the optic disc in guinea pigs was conducted using spectral-domain optical coherence tomography (SD-OCT, Heidelberg Engineering, Germany). The upper boundary of the choroid was defined as the outer surface of the retinal pigment epithelium, while the lower boundary was defined as the inner surface of the sclera (Fig. 1A). Centered on the optic disc, radial line scans

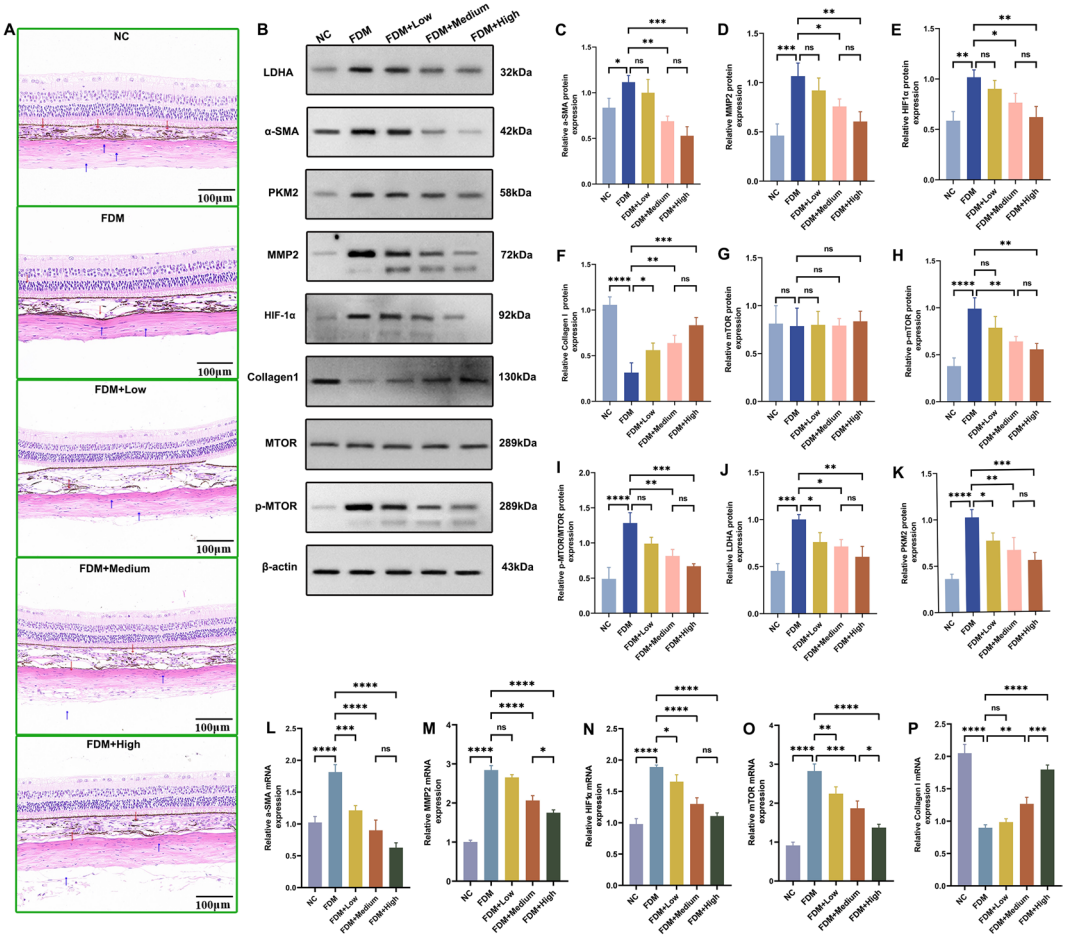

Fig. 1. (**A**) H&E-stained sections demonstrating histopathological features of the temporal posterior pole choroid/sclera following Ming's Formula intervention (Bar = 100 μm). (**B**)Western blotting was used to detect the protein levels of α-SMA (**C**), MMP2 (**D**), HIF-1α (**E**), Collagen I (**F**), mTOR (**G**), p-mTOR (**H**), p-mTOR/mTOR (**I**), LDHA (**J**) and PKM2 (**K**) in the sclera of guinea pigs 4 weeks after Ming's Formula. qPCR was used to detect the mRNA levels of α-SMA (**L**), MMP2 (**M**), HIF-1α (**N**), mTOR (**O**), and Collagen I (**P**) in the scleral tissue 4 weeks after Ming's Formula. ($n = 5$, $^{*}P < 0.05$, $^{**}P < 0.01$, $^{***}P < 0.001$, $^{****}P < 0.0001$).

were acquired along horizontal (nasal-temporal) and vertical (superior-inferior) meridians. Three concentric rings (600/1800/3600μm diameter) positioned.CT measured at 12 ring-quadrant intersections, and Choroid-sclera interface identified by automated segmentation (Heidelberg Eye Explorer). Three consecutive scans per eye; only images with quality scores > 7/10 analyzed. Arithmetic mean of qualified measurements computed as final CT.

H&E staining, and immunofluorescence staining

Three guinea pigs were randomly selected from each group for histopathological analysis 4 weeks after modeling. The guinea pigs were euthanized by intraperitoneal injection of 5% sodium pentobarbital, followed by immediate enucleation of the eyeballs. After removing the outer fascia and blood vessels, all enucleated eyeballs underwent intravitreally perfusion-fixation with Davidson's solution, followed by spatial orientation via the "superior rectus-optic nerve" dual-marker technique: superior rectus tendon suture-marked with 8 – 0 nylon and 5-mm optic nerve stump preserved as posterior pole reference. And then the intact eyeballs were immediately immersed in freshly prepared Davidson's fixative (composition: 20 ml of 40% formaldehyde, 30 ml of 95% ethanol, 10 ml of glacial acetic acid, and 30 ml of triple-distilled water) and fixed at room temperature for 3 h. The cornea and lens were carefully dissected under a microscope. Following dissection, the samples were dehydrated through a graded ethanol series, cleared in xylene, embedded in paraffin. Serial coronal Sect. (5-μm thickness) were acquired from the posterior pole within 1.5 mm on each side of the optic nerve. Sectioning proceeded along the anterior-posterior axis with superior-inferior orientation maintained. After deparaffinization and rehydration, the sections were stained with hematoxylin and eosin (H&E) and observed under an optical microscope.

The sections from each group were deparaffinized to water and subjected to antigen retrieval in a preheated EDTA antigen retrieval buffer (pH 9.0). After blocking with 3% BSA for 30 min, primary antibodies against the following proteins were added: mTOR (1:300), p-mTOR (1:500),Collagen I (1:300) and HIF-1α (1:100) followed by incubation in a humidified chamber at 4 °C overnight. After incubation, CY3-labeled species-specific secondary antibodies (1:300) were added and dark incubated at room temperature for 50 min. Next, the nuclei were counterstained with DAPI and dark incubated at room temperature for 10 min. The sections were then treated with an autofluorescence quenching agent to eliminate tissue autofluorescence and then mounted with an anti-fade mounting medium. Images were acquired using a laser-scanning confocal microscope. The channel parameters of CY3 fluorescence were as follows: excitation wavelength of 552 nm and emission wavelength of 590 nm. The channel parameters of DAPI were as follows: excitation wavelength of 358 nm and emission wavelength of 461 nm. Three random fields of view were selected for image acquisition at the same magnification (400×), and the fluorescence intensity was quantitatively analyzed using Image-Pro Plus 6.0 software.

Western blotting (WB)

Four weeks after modeling, six guinea pigs were randomly selected from each group to measure protein expression in the scleral tissue. After euthanasia, the scleral tissues were immediately isolated and placed in pre-cooled RIPA lysis buffer supplemented with 1% protease inhibitor and 1% phosphatase inhibitor. The tissue samples were ultrasonically homogenized at 4 °C and centrifuged at 12,000 rpm for 15 min. The tissues were thoroughly ground, and the supernatant was collected. The protein concentration was determined using a BCA protein quantification kit. Following denaturation, the protein samples were subjected to electrophoresis using a 10% one-step colorimetric sodium dodecyl sulfate-polyacrylamide gel (SDS-PAGE) kit to separate the target proteins. After electrophoresis, the proteins were transferred to a 0.45 μm polyvinylidene fluoride (PVDF) membrane using the wet transfer method. Following the transfer, the membrane was blocked with 5% bovine serum albumin (BSA) at room temperature for 1 h. Next. The membrane was incubated with primary antibodies (Supplemental Table 1) against a-SMA, mTOR, p-mTOR, Collagen I, HIF-1α, and MMP2 (all diluted at 1:1000), LDHA (1:5000) and PKM2 (1:2000) at 4 °C overnight. After washing with TBST, the corresponding secondary antibodies (1:300) were added and dark incubated at room temperature for 1 h. Finally, chemiluminescence detection was conducted using the FUSION-FX7 imaging system, and band intensity was analyzed using Image J. β-actin was used as the internal reference protein, and the expression level of the target proteins was determined as the ratio of the target protein to the internal reference band intensity. All experiments were conducted in triplicate to ensure the reliability of the results.

Real-time quantitative PCR

Equal amounts of scleral tissue (approximately 50 mg) from each group were homogenized using Trizol reagent, mixed with chloroform by vortexing, and centrifuged at 12,000 rpm at 4 °C for 10 min to obtain the RNA supernatant. An equal volume of isopropanol was added, mixed, and centrifuged to collect the white RNA precipitate. The precipitate was washed with 75% ethanol, air-dried at room temperature, and dissolved in 20 μL of DEPC water. The concentration and purity of RNA were evaluated using a UV spectrophotometer, and an A260/A280 ratio of 1.8-2.0 and an A260/A230 ratio > 2.0 were considered acceptable. The HiScript II Q RT SuperMix (+ gDNA wiper) reverse transcription kit was employed to obtain the cDNA of the target genes. cDNA was amplified in a 96-well plate using ChamQ Universal SYBR qPCR Master Mix. The sequence of primers is presented in Table 1. The qPCR conditions were as follows: 94 °C for 5 s for 1 cycle; 94 °C for 5 s, 54 °C for 15 s, and 72 °C for 10 s for 45 cycles. The expression levels of the target genes were normalized to the expression level of the internal reference GAPDH, and the results were analyzed using the $2-\Delta\Delta CT$ method. Information about the primer sequence is provided in Table 1.

Statistical analysis

Data were analyzed using SPSS Statistics 25.3.0 and expressed as mean ± standard deviation (SD). One-way analysis of variance (One-way ANOVA) was used to compare groups. A P-value < 0.05 was deemed statistically

Gene	Primer sequences
a-SMA	Forward: 5′-AAGAGCATCCAACCCTGCTC-3′
	Reverse: 5′-AGAGGCATAGAGGGACAGCA-3′
MMP2	Forward: 5′-GTGAAGTACGGGAATGCCGA-3′
	Reverse: 5′-CGTCTGTGCAGCTGGTGTAT-3′
MTOR	Forward: 5′-GCGTTTGTGTCCTGTTGGTC-3′
	Reverse: 5′-TGCTCCATGAACTCAGCCAG-3′
Collagen 1	Forward: 5′-TTCAGCTTTGTGGACCTCCG-3′
	Reverse: 5′-TTTCCAGGTGTCTCCGTTGG-3′
Hif1a	Forward: 5′-AGGATAAGTTCTGAACGTCGAAAAG-3′
	Reverse: 5′-ACATTGTGGGGAAGTGGCAA-3′
Gapdh	Forward: 5′-TTCTACCCACGGCAAGTTCC-3′
	Reverse: 5′-CCAGCATCACCCCACTTGAT-3′

Table 1. Primer sequences for the target genes.

significant. All statistical analyses were subjected to normality tests (Shapiro-Wilk test) and homogeneity of variance tests to ensure that data met the prerequisites for parametric tests. In addition, to get a better understanding of variables, Pearson's product-moment correlation coefficients (R) were calculated to assess the linear relationships between variables.

Results

Mingshi formula attenuated refractive error and axial elongation in FMD

Before myopia induction, there were no significant differences in refractive error and axial length of the right eye between the NC group and other groups (all $P > 0.05$) (Fig. 2A and B). However, after 4 weeks of myopia induction, the FDM group exhibited a significant increase in refractive error ($P < 0.001$) and axial elongation ($P < 0.001$) compared to the NC group. Notably, compared to the FDM group, the FDM + High group significantly controlled myopia, with a $P < 0.01$ for both refractive error and axial length. Although there were significant differences between the high-dose group and the NC group, their magnitude of change was significantly lower than that of the FDM group (both $P < 0.01$). The results indicated that treatment with Ming's Formula effectively decelerated the progression of FDM.

Mingshi formula attenuated choroidal thinning in FDM

FDM can change choroidal morphology. We measured the choroidal thickness of guinea pigs in each group before and after inducing myopia to systematically measure the effects of FDM on choroidal morphology and the therapeutic effects of Ming's Formula. There were no significant differences in choroidal thickness among the groups before inducing myopia (Fig. 2C). After 4 weeks of treatment, the FDM group showed significant choroidal thinning compared to the NC group, with decreased choroidal thickness (Fig. 2D. $P < 0.001$). Although the choroidal thickness in the Ming's Formula groups increased compared to the FDM group, it was still significantly lower than that in the NC group ($P < 0.01$). This finding indicates that Ming's Formula partly mitigated choroidal thinning.

Mingshi formula alleviated the structural abnormalities of the choriod and sclera in FDM

H&E staining was conducted on the eyeballs of each group 4 weeks after inducing myopia to investigate the effects of Ming's Formula on the morphology of the choroid and sclera in myopic guinea pigs (Fig. 1A). The NC group exhibited a densely arranged choroidal structure with an intact and compact capillary network. The sclera displayed a typical three-layer structure (superficial, middle, and deep layers) with regularly arranged collagen fibers. In contrast, the FDM group exhibited significant pathological changes: the choroidal stroma was loose, the structural arrangement was disorganized, the integrity of the capillary network was disrupted, and the vascular density was reduced. The sclera was thinner, with a disordered arrangement of collagen fibers and a blurred layered structure. Notably, the Ming's Formula groups exhibited dose-dependent histological improvements. Compared to the FDM group, all dose groups showed increased vascular density and more medium and large blood vessels in the choroid. The collagen fibers in the sclera were more regularly arranged, and the layered structure was significantly improved, with the high-dose group showing structural similarity to the NC group. These results indicate that Ming's Formula can effectively ameliorate myopia-induced choroidal thinning and scleral structural disorganization, reversing pathological changes associated with myopia.

The Mingshi formula inhibited the mTOR/HIF-1α signaling pathway to attenuate the progression of FDM

After 4 weeks of myopia induction, the FDM group exhibited significant molecular changes compared to the NC group (Fig. 1), including upregulation of mTOR expression, increased expression of its downstream target HIF-1α, and enhanced expression of fibrosis markers α-SMA and MMP2 ($P < 0.001$, Fig. 1.L, M). However, the expression of Collagen I, a major component of the extracellular matrix, was significantly downregulated in this group ($P < 0.001$). These findings suggest that the mTOR/HIF-1α signaling pathway is significantly

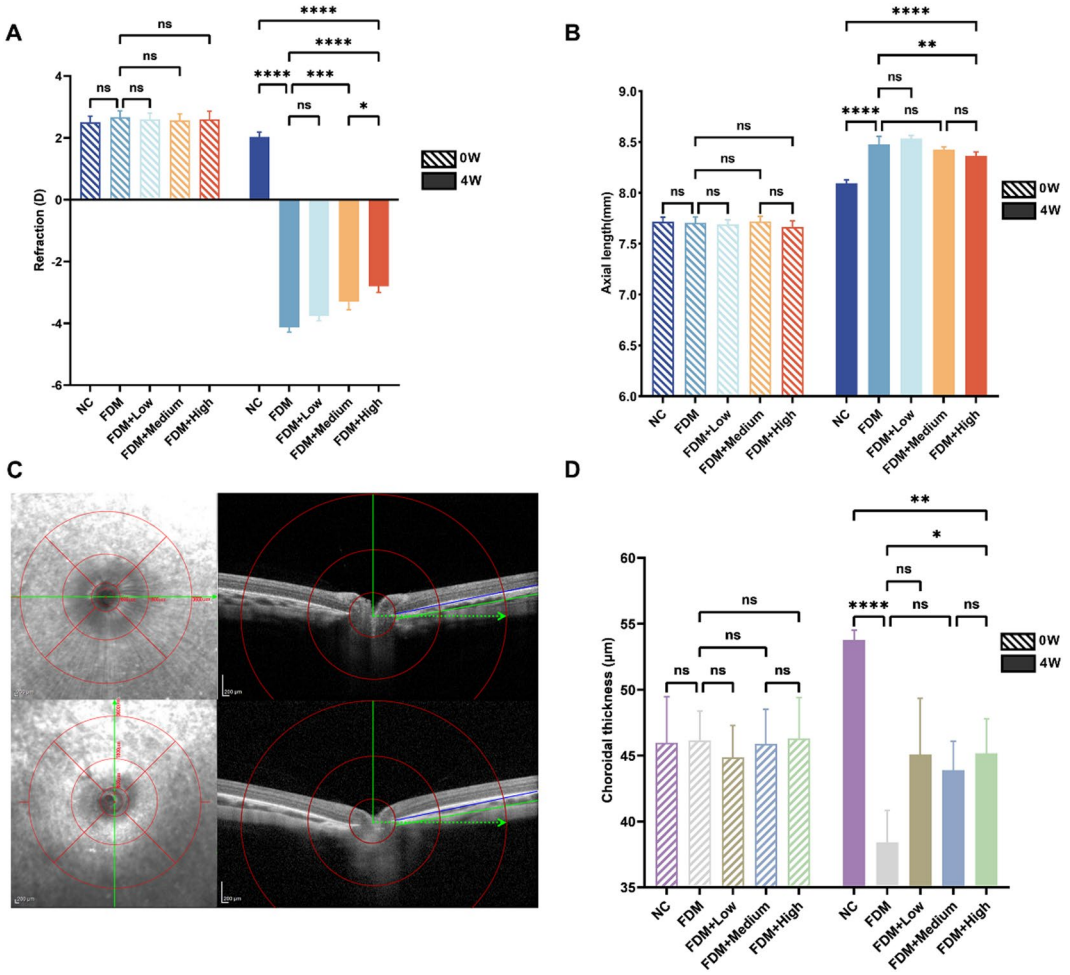

Fig. 2. Refraction (**A**) and axial length (**B**) of guinea pigs in the NC, FDM, FDM + Low, FDM + Medium, and FDM + High groups were measured before inducing myopia and 4 weeks after inducing myopia ($n = 75$, $^{**}P < 0.01$, $^{***}P < 0.001$, $^{****}P < 0.0001$). Schematic diagram of ChT measurement. (**C**) Fundus analysis using OCT and captured structural images of guinea pigs showing the defined regions: red lines indicate the inner concentric circle (600 μm, green arrow), middle concentric circle (1800 μm, green arrow), and outer concentric circle (3600 μm, green arrow). The optic disc is defined as the center, and the choroidal layer boundaries are located between the two green-blue lines. (**D**) Analysis of choroidal thickness in each group of guinea pigs ($n = 10$, $^{*}P < 0.05$, $^{**}P < 0.01$, $^{****}P < 0.0001$).

activated during scleral remodeling in myopia. Notably, the Ming's Formula groups dose-dependently reversed these molecular alterations. Compared to the FDM group, the expression of genes activated by the mTOR/HIF-1α pathway was downregulated in all Ming's Formula groups ($P < 0.01$, 0.001, Fig. 1.O). The high-dose group showed no significant difference in HIF-1α expression compared to the NC group ($P > 0.05$, Fig. 1.N), and a significant recovery was observed in Collagen I expression ($P < 0.001$, Fig. 1.P). The results indicated that Ming's Formula alleviated the hypoxic microenvironment of the sclera, inhibited pathological fibrosis, and regulated matrix remodeling by modulating the mTOR-HIF-1α signaling axis, thereby delaying the progression of myopia.

Mingshi formula inhibited the mTOR-HIF-1α signaling pathway to prevent the progression of FDM

Consistent with the gene expression levels of mTOR, HIF-1α, α-SMA, MMP2, and Collagen I, compared to the NC group, the protein expression levels of HIF-1α, α-SMA, MMP2, LDHA and PKM2 in the sclera were significantly upregulated 4 weeks after myopia induction, while the expression of Collagen I showed a downward trend (Fig. 1B). Notably, the phosphorylation level of mTOR was significantly enhanced ($P < 0.0001$, Fig. 1G–I), indicating that the p-mTOR was markedly activated in the sclera of guinea pigs with FDM. Compared to the FDM group, the sclera of guinea pigs in the Ming's Formula groups exhibited a dose-dependent inhibition of this signaling pathway ($P < 0.05$, 0.01, 0.001). Based on these findings, we speculated that Ming's Formula may inhibit mTOR phosphorylation, thereby downregulating HIF-1α expression, improving scleral hypoxia, preventing fibrosis, regulating ECM remodeling, and delaying the progression of myopia.

We conducted immunofluorescence staining on the eye sections of guinea pigs after 4 weeks of myopia induction to validate the aforementioned molecular mechanisms. The expression of Collagen I was reduced in

the sclera of myopic guinea pigs (Fig. 3A), while the expression of HIF-1α was enhanced (Fig. 3B), with greater staining intensity indicating aggravated hypoxia (Fig. 3.E, F, $P < 0.001$). Simultaneously, mTOR phosphorylation was significantly enhanced (Fig. 3C, D, G, H), suggesting the activation of this signaling pathway. In contrast, the scleral tissue of guinea pigs in the Ming's Formula groups exhibited mild hypoxia, reduced mTOR phosphorylation, and increased Collagen I expression. These results confirm that the progression of myopia is accompanied by mTOR phosphorylation and more severe scleral hypoxia. Our findings also revealed that treatment with Ming's Formula can effectively mitigate these pathological changes. This finding is highly consistent with the results of previous molecular experiments, suggesting that Ming's Formula protects against myopia by regulating the mTOR-HIF-1α signaling pathway.

Moreover, correlation analyses was conducted, which demonstrated significant associations between refractive shift and expression levels of HIF-1α, Collagen I, MMP-2, p-mTOR, LDHA, and PKM2, as well as between HIF-1α and the glycolytic enzymes LDHA and PKM2 (all $p < 0.01$, Fig. 4).

mTOR Inhibition enhances the therapeutic efficacy of MingShi formula in delaying myopia progression

H&E staining revealed comparable choroidal and scleral morphology between mTOR inhibitor-treated and high-dose Ming's formulagroups (Fig. 5.A).The NC group exhibited a tightly organized choroidal structure with an intact, dense capillary network and regularly arranged scleral collagen fibers.In contrast, FDM group displayed loose choroidal stroma, disorganized architecture, compromised capillary integrity, disordered

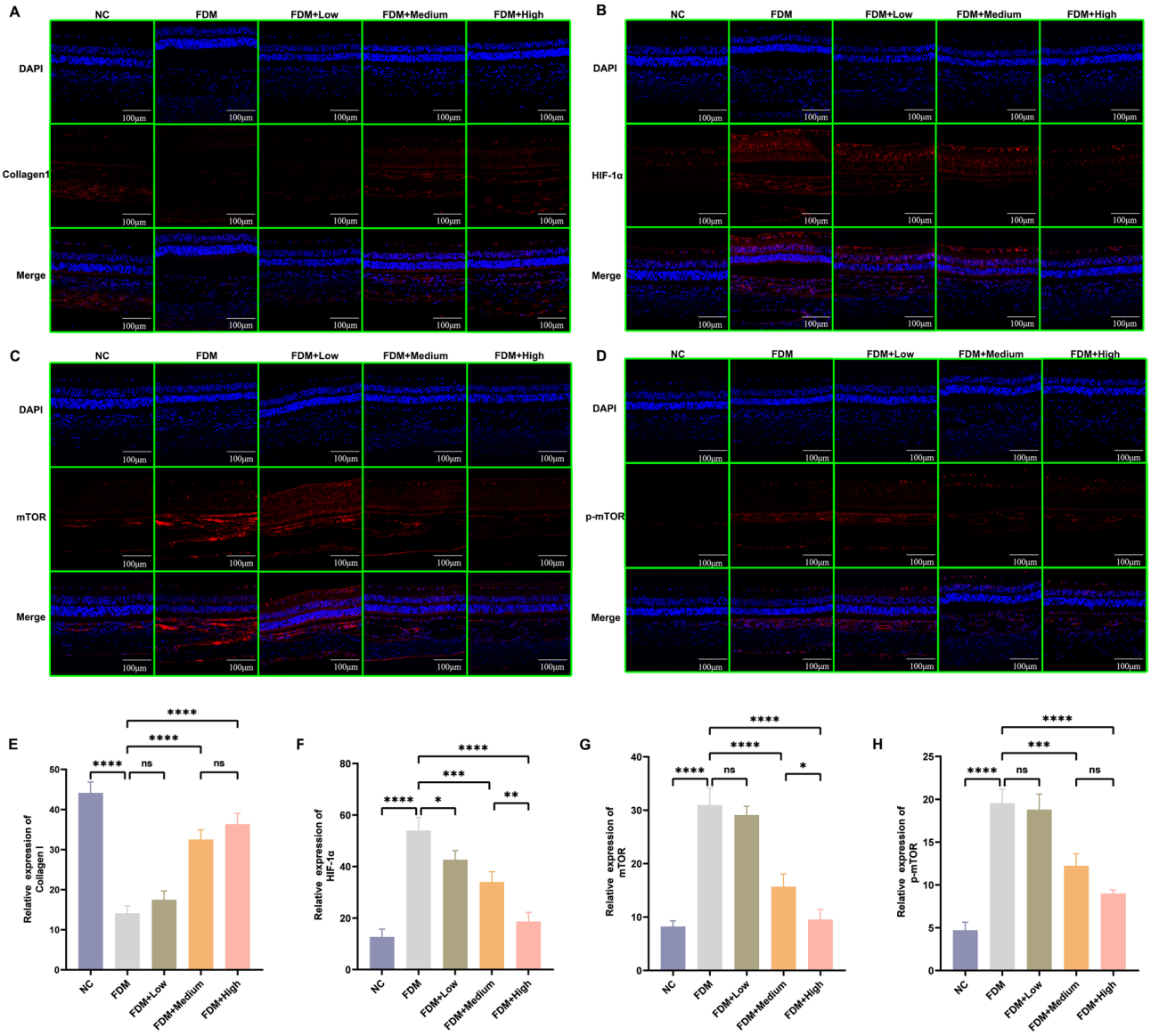

Fig. 3. Immunofluorescence detection of Collagen I (**A**), mTOR (**B**), HIF-1α (**C**) and p-mTOR (**D**) in temporal posterior pole sclera across groups, with corresponding quantitative analyses (**E**–**H**) ($n = 3$, $^{*}P < 0.05$, $^{**}P < 0.01$, $^{***}P < 0.001$, $^{****}P < 0.0001$). Bar = 100 μm.

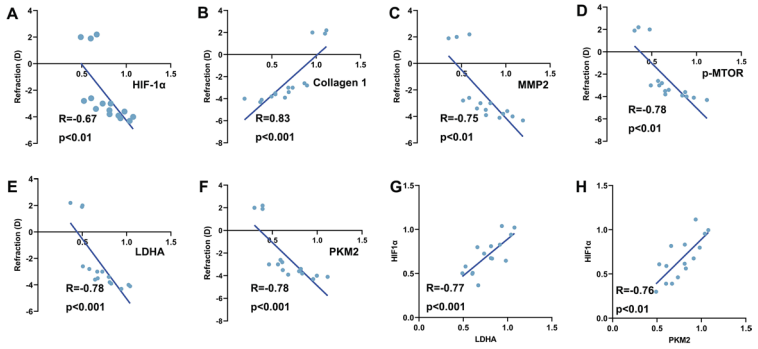

Fig. 4. Correlation analysis of refractive shift with HIF-1α (**A**), Collagen I (**B**), MMP2 (**C**), p-mTOR (**D**), LDHA (**E**), and PKM2 (**F**), as well as HIF-1α with LDHA (**G**) and PKM2 (**H**).

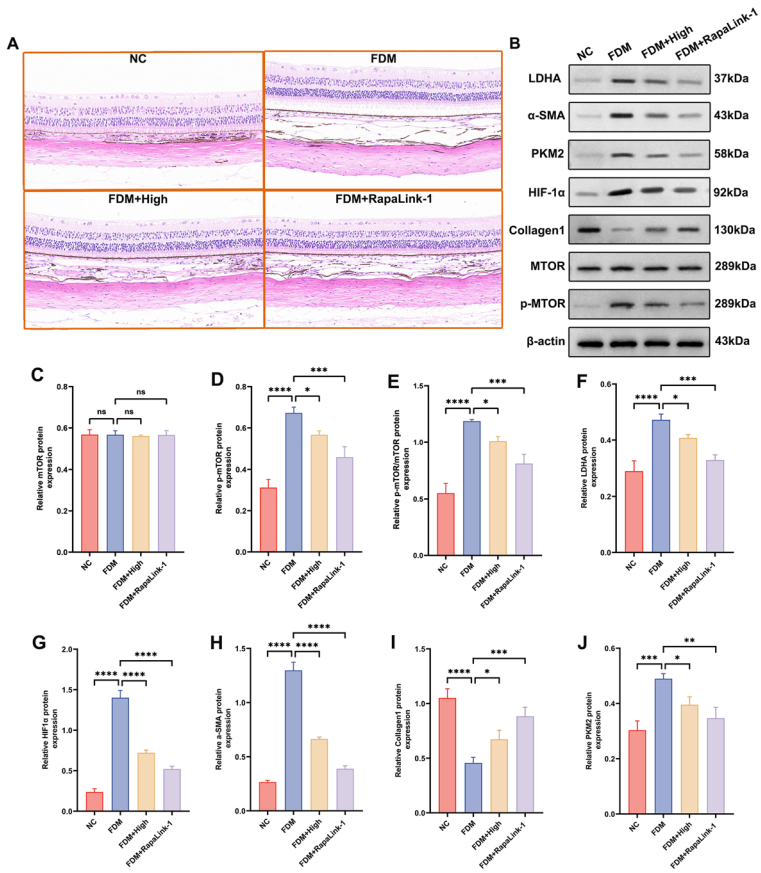

Fig. 5. (**A**) H&E staining of ocular tissue sections showing the histopathological features of the temporal posterior pole choroid/sclera in guinea pigs after MTOR inhibitor (Bar = 100 μm). (**B**) Western blotting was used to detect the protein levels of mTOR (**C**), p-mTOR (**D**), p-mTOR/MTOR (**E**), LDHA (**F**), HIF-1α (**G**), α-SMA (**H**), Collagen I (**I**) and PKM2 (**J**) in the sclera of guinea pigs after MTOR inhibitor ($n = 3$, $^{*}P < 0.05$, $^{**}P < 0.01$, $^{***}P < 0.001$, $^{****}P < 0.0001$).

collagen fiber arrangement, and blurred lamellar structures. Relative to the FDM group, mTOR inhibitor treatment increased choroidal vascular density, restored regular collagen fiber alignment– with high-dose Ming's formula demonstrating comparable restorative effects.

Western blot analysis demonstrated significantly enhanced mTOR phosphorylation ($P < 0.001$) in the FDM group versus NC (Fig. 5B, C, D, E), accompanied by upregulated HIF-1α, α-SMA, MMP-2, LDHA, and PKM2 expression alongside decreased Collagen I levels (Fig. 5F, G, H, I, J). mTOR inhibition significantly attenuated phosphorylation, downregulated these hypoxia-responsive proteins, and elevated Collagen I expression. Collectively, these results indicate mTOR inhibition synergistically potentiates Ming's formula by modulating the mTOR/HIF-1α signaling axis to delay myopia progression.

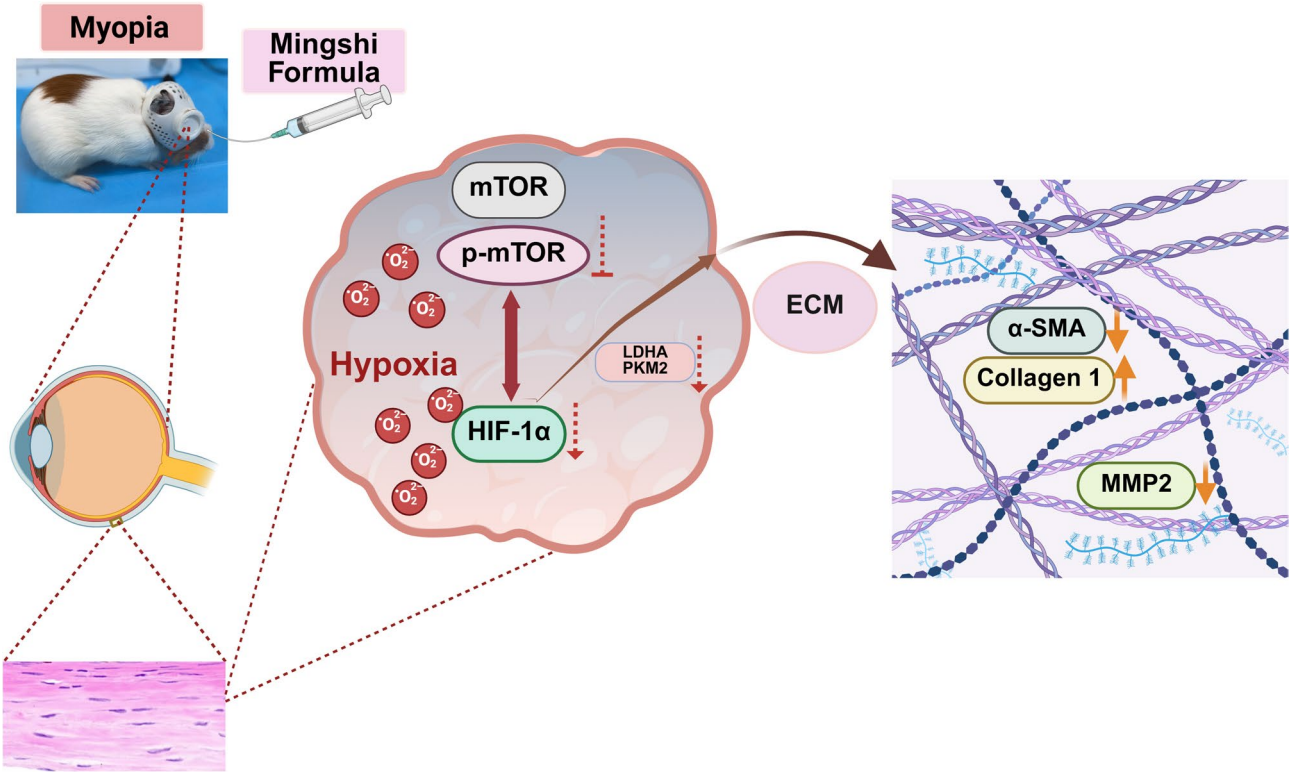

Fig. 6. Ming's formula modulates the mTOR/HIF-1α signaling pathway by targeting mTOR to inhibit its phosphorylation and downregulate HIF-1α expression. This intervention ameliorates the hypoxic scleral microenvironment, corrects dysregulated collagen synthesis, reverses pathological ECM remodeling, and ultimately attenuates myopia progression in FDM guinea pigs.

Discussion

This study demonstrates that Ming's Formula modulates scleral metabolic homeostasis through coordinated inhibition of mTOR phosphorylation (p-mTOR Ser2448) and disruption of HIF-1α transcriptional complex formation. Specifically, the formula suppresses HIF-1α-driven glycolytic enzymes (LDHA/PKM2), alleviates scleral hypoxia, normalizes expression of ECM regulators (MMP2/Collagen 1/α-SMA), and attenuates pathological ECM remodeling.Collectively, these actions decelerate form-deprivation myopia progression in guinea pigs.These findings delineate a previously unrecognized mechanism wherein Ming's Formula delays myopia progression via mTOR/HIF-1α-mediated metabolic reprogramming, providing mechanistic insights for novel antimyopia strategies targeting scleral hypoxia (Fig. 6).

mTOR, as a serine/threonine kinase, dynamically integrates nutrient signals, growth factor stimulation, and cellular energy status through its phosphorylation site (Ser2448), serving as a key regulator of cell cycle and metabolic homeostasis[11,12]. Its abnormal activation can drive abnormal scleral fibroblast proliferation[13], and lead to ECM metabolic imbalance by upregulating MMP2 expression and inhibiting Collagen I synthesis[14], finally resulting in scleral thinning and pathological axial elongation[2]. Reduced choroidal blood flow and decreased capillary density and thinning induce HIF-1α expression in the hypoxic microenvironment of the sclera in myopia, which regulates the transcription of genes, such as Collagen I and MMP-2, forming a positive feedback loop that promotes ECM remodeling[15]. Notably, previous studies have primarily focused on the unidimensional regulatory role of HIF-1α, overlooking its interaction with the mTOR signaling network. This study provides evidence supporting the role of the mTOR/HIF-1α signaling axis in scleral hypoxia. For the first time, we report that Ming's formuladownregulates scleral HIF-1α expression by 2.0-fold, a reduction significantly correlated with decreased expression of the glycolytic genes LDHA and PKM2. Furthermore, mTOR inhibition downregulates HIF-1α expression, alleviates the hypoxic scleral microenvironment, reduces metabolite accumulation, and attenuates scleral extracellular matrix remodeling and axial elongation. This finding is consistent with the results of Cheng JW et al.[16, 17], further expanding our understanding of the regulatory network of mTOR in myopia and clarifying the importance of HIF-1α as an upstream regulatory factor. Furthermore, prior studies demonstrate that scleral hypoxia induces upregulation of MMP-2 and Collagen I, thereby promoting myopia progression[18]. This study establishes that Ming's formula concurrently downregulates HIF-1α, MMP-2, and Collagen I, demonstrating its capacity to block the hypoxia-induced matrix degradation pathway, thereby inhibiting myopia development.

Currently, rapamycin, as a classic mTOR inhibitor, has been widely used to study the role of the mTOR signaling pathway in the pathological progression of myopia[19]. However, preclinical studies have shown that long-term treatment with rapamycin may cause severe side effects[20], such as immunosuppression[21] (imbalance

in CD4+/CD8 + T cell ratios) and metabolic disorders[22] (e.g., reduced insulin sensitivity and abnormal lipid metabolism)[23]. We confirmed that Ming's Formula can significantly decrease mTOR Ser2448 phosphorylation, downregulate HIF-1α expression, alleviate scleral hypoxia, and maintain the normal cross-linking of scleral collagen fibers. Although Ming's Formula inhibited the excessive activation of the mTOR signaling pathway, it did not significantly affect the physiological metabolic activity of scleral fibroblasts or collagen homeostasis. This characteristic aligns closely with the "multi-component, multi-target, multi-pathway" synergistic regulation theory proposed by Zhao et al.[24], significantly lowering the risk of adverse reactions associated with single-target inhibitors while maintaining therapeutic efficacy[25]. Based on these findings, Ming's Formula possesses significant advantages as a novel anti-myopia drug, and its multi-target regulatory properties provide a new research direction for developing efficient and safe strategies for preventing and controlling myopia. In addition, all histological analyses were performed on standardized posterior pole regions (≤ 1.5 mm from optic nerve head), the principal site of myopic scleral remodeling exhibiting maximal pathological changes[26]. The dual-marker protocol (superior rectus suture + optic nerve stump) guaranteed spatial consistency across specimens (positional error < 50 μm), confirming that observed structural variations represent true biological effects rather than sectioning-induced deformations.

Although this study revealed the mechanism by which Ming's Formula delays the progression of myopia through the mTOR/HIF-1α signaling pathway, there are still some limitations. First, the experimental model was limited to guinea pigs with FDM, and future studies are needed to validate the generalizability of the findings in other animals, such as tree shrews and rhesus monkeys, whose visual systems are more similar to the human visual system. Second, as a multi-component traditional Chinese medicine compound, the specific targets and pharmacokinetic characteristics of its active ingredients (e.g. ginsenosides and pachymic acid) have not been fully elucidated. Further analyses based on ultra-high-performance liquid chromatography-tandem mass spectrometry and molecular docking techniques are needed to decipher its "component-target-pathway" network. Finally, Quantify scleral hypoxia resolution through in vivo oxygen tension mapping. Establish causal necessity using HIF-1α-knockdown scleral fibroblasts. Future studies should integrate multi-omics technologies to comprehensively analyze the role of the mTOR/HIF-1α signaling pathway in myopia, providing robust evidence for the precise treatment of myopia.

Conclusion

This study demonstrates that Ming's formula inhibits phosphorylation of mTOR at Ser2448 and downregulates HIF-1α expression.Through targeted modulation of the mTOR/HIF-1α signaling axis, it ameliorates the hypoxic scleral microenvironment, rebalances collagen synthesis, reverses pathological extracellular matrix remodeling, and collectively delays myopia progression. Collectively, these findings advance the theoretical framework for traditional Chinese medicine compounds in myopia treatment via characteristic "multi-target, multi-pathway" mechanisms, while providing pharmacological evidence and potential targets for novel anti-myopia therapeutics.

Data availability

All data generated or analysed during this study are included in this published article and its supplementary information files.

Received: 10 March 2025; Accepted: 18 September 2025
Published online: 24 October 2025

References

1. Sun, J. et al. Rising prevalence of myopia and high myopia in Chinese adolescents: A 10-year longitudinal study. *JAMA Ophthalmol.* **138** (5), 505–512 (2020).
2. Wu, H. et al. Scleral hypoxia is a target for myopia control. *Proc. Natl. Acad. Sci. U S A.* **115** (30), E7091–e100. https://doi.org/10.1073/pnas.1721443115 (2018).
3. Zhang, L. et al. Palladium nanocrystals regulates scleral extracellular matrix remodeling in myopic progression by modulating the hypoxia signaling pathway Nrf-2/Ho-1. *J. Control Release.* **373**, 293–305. https://doi.org/10.1016/j.jconrel.2024.07.031 (2024).
4. Kubaichuk, K. & Kietzmann, T. USP10 contributes to colon carcinogenesis via mTOR/S6K mediated HIF-1α but not HIF-2α protein synthesis. *Cells* **12** (12), 1585. https://doi.org/10.3390/cells12121585 (2023).
5. Han, W. et al. Inhibition of the mTOR pathway exerts cardioprotective effects partly through autophagy in CLP rats. *Mediators Inflamm.* **2018**, 4798209. https://doi.org/10.1155/2018/4798209 (2018).
6. Wang, J. et al. Mingshi formula for low myopia in children with heart Yang insufficiency syndrome: A multicentre, double-blind, randomised placebo-controlled study. *J. Tradit Chin. Med.* **65** (6), 587–593. https://doi.org/10.13288/j.11-2166/r.2024.06.008 (2024).
7. Cao, K. E. Study on mechanism of Mingshi prescription in preventing and controlling myopia based on scleral untargeted metabolomics [Doctoral dissertation]. *Beijing: China Acad. Chin. Med. Sci.* (2023).
8. Zeng, X. et al. Synergistic anti-tumour activity of ginsenoside Rg3 and doxorubicin on proliferation, metastasis and angiogenesis in osteosarcoma by modulating mTOR/HIF-1α/VEGF and EMT signalling pathways. *J. Pharm. Pharmacol.* **75** (11), 1405–1417. https://doi.org/10.1093/jpp/rgad070 (2023).
9. Qin, G. W., Lu, P., Peng, L. & Jiang, W. Ginsenoside Rb1 inhibits cardiomyocyte autophagy via PI3K/Akt/mTOR signaling pathway and reduces myocardial Ischemia/Reperfusion injury. *Am. J. Chin. Med.* **49** (8), 1913–1927. https://doi.org/10.1142/S0192415X21500907 (2021).
10. Li, X., Zhu, Q., Liu, Y., Yang, Z. & Li, B. Gastrodin protects myocardial cells against hypoxia/reoxygenation injury in neonatal rats by inhibiting cell autophagy through the activation of mTOR signals in PI3K-Akt pathway. *J. Pharm. Pharmacol.* **70** (2), 259–267. https://doi.org/10.1111/jphp.12838 (2018).
11. Liu, G. Y. & Sabatini, D. M. mTOR at the nexus of nutrition, growth, ageing and disease. *Nat. Rev. Mol. Cell. Biol.* **21** (4), 183–203. https://doi.org/10.1038/s41580-019-0199-y (2020).
12. Panwar, V. et al. Multifaceted role of mTOR (mammalian target of rapamycin) signaling pathway in human health and disease. *Signal. Transduct. Target. Ther.* **8** (1), 375. https://doi.org/10.1038/s41392-023-01608-z (2023).

13. Karonitsch, T. et al. mTOR senses environmental cues to shape the fibroblast-like synoviocyte response to inflammation. *Cell. Rep.* **23** (7), 2157–2167. https://doi.org/10.1016/j.celrep.2018.04.044 (2018).
14. Igarashi, N., Honjo, M. & Aihara, M. Effects of mammalian target of Rapamycin inhibitors on fibrosis after trabeculectomy. *Exp. Eye Res.* **203**, 108421. https://doi.org/10.1016/j.exer.2020.108421 (2021).
15. Zhang, S. et al. Changes in choroidal thickness and choroidal blood perfusion in Guinea pig myopia. *Invest. Ophthalmol. Vis. Sci.* **60** (8), 3074–3083. https://doi.org/10.1167/iovs.18-26397 (2019).
16. Cheng, J. W. et al. Berberine ameliorates collagen-induced arthritis in mice by restoring macrophage polarization via AMPK/mTORC1 pathway switching glycolytic reprogramming. *Int. Immunopharmacol.* **124** (Pt B), 111024. https://doi.org/10.1016/j.intimp.2023.111024 (2023).
17. Cam, H., Easton, J. B., High, A. & Houghton, P. J. mTORC1 signaling under hypoxic conditions is controlled by ATM-dependent phosphorylation of HIF-1α. *Mol. Cell.* **40** (4), 509–520. https://doi.org/10.1016/j.molcel.2010.10.030 (2010).
18. Wu, W. et al. Hypoxia-Induced scleral HIF-2α upregulation contributes to rises in MMP-2 expression and myopia development in mice. *Invest. Ophthalmol. Vis. Sci.* **63** (8), 2. https://doi.org/10.1167/iovs.63.8.2 (2022).
19. Zhang, R. et al. mTORC1 signaling and negative lens-induced axial elongation. *Invest. Ophthalmol. Vis. Sci.* **64** (10), 24. https://doi.org/10.1167/iovs.64.10.24 (2023).
20. Kabaklıoğlu, M. et al. Short- and long-term effects of Rapamycin on ischemic damage and apoptotic changes in torsion of rat testes. *Naunyn Schmiedebergs Arch. Pharmacol.* **394** (1), 85–94. https://doi.org/10.1007/s00210-020-01965-4 (2021).
21. Cortazar, F. et al. Clinical outcomes in kidney transplant recipients receiving long-term therapy with inhibitors of the mammalian target of Rapamycin. *Am. J. Transpl.* **12** (2), 379–387. https://doi.org/10.1111/j.1600-6143.2011.03826.x (2012).
22. Isakova, T. et al. Inhibitors of mTOR and risks of allograft failure and mortality in kidney transplantation. *Am. J. Transpl.* **13** (1), 100–110. https://doi.org/10.1111/j.1600-6143.2012.04281.x (2013).
23. Fang, Y. et al. Duration of Rapamycin treatment has differential effects on metabolism in mice. *Cell. Metab.* **17** (3), 456–462. https://doi.org/10.1016/j.cmet.2013.02.008 (2013).
24. Zhao, M., Che, Y., Gao, Y. & Zhang, X. Application of multi-omics in the study of traditional Chinese medicine. *Front. Pharmacol.* **15**, 1431862. https://doi.org/10.3389/fphar.2024.1431862 (2024).
25. Liu, L. et al. Mechanism of Chinese botanical drug Dizhi pill for myopia: an integrated study based on bioinformatics and network analysis. *Med. (Baltim).* **102** (38), e34753. https://doi.org/10.1097/md.0000000000034753 (2023).
26. McBrien, N. A., Lawlor, P. & Gentle, A. Scleral remodeling during the development of and recovery from axial myopia in the tree shrew. *Invest. Ophthalmol. Vis. Sci.* **41** (12), 3713–3719 (2000).

Acknowledgements

The authors thank the members of their laboratory and their collaborators for their support. The authors would like to express their gratitude to EditSprings (https://www.editsprings.cn) for the expert linguistic services provided.

Author contributions

Yixue Yin: Validation, Formal Analysis, Investigation, Writing Original Draft; Xiuyan Zhang: Formal Analysis; Yibo Han: Investigation; Jike Song: Conceptualization, Writing Review & Editing, Fund Acquisition; Hongsheng Bi: Conceptualization, Writing Review & Editing.

Funding

This work was supported by the Shandong Provincial Natural Science Foundation (No. ZR2021LZY045), Shandong Provincial Key Research and Development Program (No.2021LCZX09) and Traditional Chinese Medicine Science and Technology Project of Shandong Province (No. Q-2023015). The funders had no role in study design, data collection and analysis, the decision to publish, or the preparation of the manuscript.

Declarations

Competing interests

The authors declare no competing interests.

Ethics approval and consent to participate

The experimental protocol was established following the ethical guidelines of the Association for Research in Vision and Ophthalmology (ARVO) and was approved by the Animal Ethics Committee of the Affiliated Hospital of Shandong University of Traditional Chinese Medicine (Approval No.:2023010).

Consent for publication

All data collected in this study are included in the article.

Additional information

Supplementary Information The online version contains supplementary material available at https://doi.org/10.1038/s41598-025-21085-4.

Correspondence and requests for materials should be addressed to J.S. or H.B.